Observational Study

Medicine®

OPEN

# Clinical value of texture analysis in differentiation of urothelial carcinoma based on multiphase computed tomography images

Zihua Wang, MS[a,b], Yufang He, MS[a], Nianhua Wang, MD[a], Ting Zhang, BS[a], Hongzhen Wu, MD[a,*], Xinqing Jiang, MD[a,b,*], Lei Mo, BS[a,b,*]

**Abstract**

Identification of histologic grading of urothelial carcinoma still depends on histopathologic examination. As an emerging and promising imaging technology, radiomic texture analysis is a noninvasive technique and has been studied to differentiate various tumors. This study explored the value of computed tomography (CT) texture analysis for the differentiation of low-grade urothelial carcinoma (LGUC), high-grade urothelial carcinoma (HGUC), and their invasive properties.

Radiologic data were analyzed retrospectively for 94 patients with pathologically proven urothelial carcinomas from November 2016 to April 2019. Pathologic examination demonstrated that tumors were: high grade in 43 cases, and low grade in 51 cases; and nonmuscle invasive (NMI) in 37 cases, and muscle invasive (MI) in 37 cases. Maximum tumor diameters on CT scan were manually outlined as regions of interest and 78 texture features were extracted automatically. Three-phasic CT images were used to measure texture parameters, which were compared with postoperative pathologic grading and invasive results. The independent sample *t* test or Mann–Whitney *U* test was used to compare differences in parameters. Receiver-operating characteristic curves for statistically significant parameters were used to confirm efficacy.

Of the 78 features extracted from each phase of CT images, 26 (33%), 20 (26%), and 22 (28%) texture parameters were significant ($P < .05$) for differentiating LGUC from HGUC, while 19 (24%), 16 (21%), and 30 (38%) were significant ($P < .05$) for differentiating NMI from MI urothelial carcinoma. Highest areas the under curve for differentiating grading and invasive properties were obtained by variance (0.761, $P < .001$) and correlation (0.798, $P < .001$) on venous-phase CT images.

Texture analysis has the potential to distinguish LGUC and HGUC, or NMI from MI urothelial carcinoma, before surgery.

**Abbreviations:** AUC = area under curve, CT = computed tomography, DP = delayed phase, GLCM = gray-level co-occurrence matrix, HGUC = high-grade urothelial carcinoma, LGUC = low-grade urothelial carcinoma, MI = muscle invasive, NMI = nonmuscle invasive, MIUC = muscle-invasive urothelial carcinoma, NMIUC = nonmuscle-invasive urothelial carcinoma, ROC = receiver-operating characteristic, ROI = region of interest, VP = venous phase.

**Keywords:** bladder cancer, computed tomography, radiomics, texture analysis, urothelial carcinoma

## 1. Introduction

Urothelial carcinoma (UC), the most common histologic type of bladder cancer, is the tenth most common malignancy worldwide, with an increasing incidence, especially in men.[1] According to the differentiated extent of tumor cells, UC can be graded as low grade (LG) or high grade (HG), and this grading is significant for assessing UC because well-differentiated (LG) carcinomas are less aggressive than HGUC.[2,3] In addition, UC is divided into nonmuscle invasive (NMI) and muscle invasive (MI) based on the 2016 WHO classification of tumors of the urinary

*Editor: Giuseppe Lucarelli.*

*This study was supported by the Science Foundation of Guangzhou First People's Hospital (No. M2019013) and the Science and Technology Planning Project of Guangzhou (No. 201510010086, 201904010422).*

*This study was received the approval by the ethics committees of Guangzhou First People's Hospital (K-2020-005-01). This study was conducted in accordance with the principles outlined in the Declaration of Helsinki. Informed consent was not necessary, because the data are anonymized.*

*The authors have no conflicts of interest to disclose.*

*Supplemental Digital Content is available for this article.*

*All data generated or analyzed during this study are included in this published article [and its supplementary information files].*

*[a] Department of Radiology, Guangzhou First People's Hospital, School of Medicine, South China University of Technology, [b] Department of Radiology, Guangzhou First People's Hospital, Guangzhou Medical University, Guangzhou, Guangdong, China.*

*[*] Correspondence: Lei Mo, Xinqing Jiang and Hongzhen Wu, Department of Radiology, Guangzhou First People's Hospital, School of Medicine, South China University of Technology, Guangzhou, Guangdong 510180, China, Guangzhou First People's Hospital, Guangzhou Medical University, Guangzhou 510180, China (e-mail: eymolei@scut.edu.cn, eyjiangxq@scut.edu.cn, and eywuhongzhen@scut.edu.cn).*



*How to cite this article: Wang Z, He Y, Wang N, Zhang T, Wu H, Jiang X, Mo L. Clinical value of texture analysis in differentiation of urothelial carcinoma based on multiphase computed tomography images. Medicine 2020;99:18(e20093).*

*Received: 1 October 2019 / Received in final form: 7 March 2020 / Accepted: 1 April 2020*

*http://dx.doi.org/10.1097/MD.0000000000020093*

system.[4] Researchers[2,5] showed that depth of tumor invasion into the wall of the urinary bladder is an independent prognostic factor, and the implications of histopathology (LG or HG) for UC diagnosis, prognosis, and treatment are explicit. Therefore, identification of histologic grading of UC is needed to identify patients likely to benefit from preoperative diagnosis. However, the final diagnosis still depends on histopathologic examination. As an invasive examination method, biopsy still has the problems of misdiagnosis or misclassification during preoperative diagnosis because of inadequate specimens or variability in pathologic features.[6]

Computed tomography (CT) is the imaging modality widely used for tumor staging, and for monitoring recurrence during clinical diagnosis. However, it is challenging for radiologists to identify the pathologic grading and invasive properties of UC with CT images.

As an emerging and promising imaging technology, radiomic texture analysis is a noninvasive technique of high-throughput extraction of quantitative imaging data and has been studied to differentiate various tumors and predict responses to chemotherapy in patients with carcinoma.[7–13] Texture analysis could be implemented to describe correlations between the grey level intensity of pixels or voxels, their positions within an image for evaluating intratumoral heterogeneity and extracting data about pixel spatial intensity variations across lesions of interest.[14] Previous studies[15–18] used CT texture analysis to distinguish the different grades and aggressiveness of bladder cancer.

The purpose of this study was to determine whether more significant texture feature parameters on multiphase CT scan images acquired before surgery are independently related to pathologic grading and invasive properties in patients with UC.

## 2. Materials and methods

### 2.1. Patient selection

Patients confirmed with UC, from our hospital databases between November 2016 and February 2019, were identified. Patients had undergone a CT scan of the abdomen and pelvis with intravenous contrast, and pathology results were also available. A total of 112 patients were included, with UC proven by pathologic diagnosis after surgical resection. Patients with tumors smaller than 5 mm (n = 6) and bladder wall thickening without mass (n = 3) were excluded to ensure enough lesion area for drawing regions of interest (ROI). Three patients were excluded because of images with metallic or motion artifacts. To reduce the effects of image-density disparities and to minimize confounding factors, 6 patients with huge masses were also excluded, because the tumors showed markedly different enhancement from other lesions. Overall, 90 patients had single tumors, and in the remaining 4 patients with multiple lesions, the largest lesion was selected.

The grade of UC was divided into LGUC and HGUC, stage of UC was divided into NMIUC and MIUC. The study population consisted of 94 patients according to grade (group 1: 43 LG vs 51 HG) and 74 patients according to stage (group 2: 37 NMI vs 37 MI), because 20 lesions did not have pathologic results for stage. Inclusion and exclusion criteria and sample size are shown in Figure 1. Clinical information was reviewed retrospectively from electronic health records. No patient received chemotherapy or radiotherapy before surgery. A total of 91 tumors were 1st lesions, while subjects with recurrent lesions were divided into groups according to their latest pathology results.

This study was approved by the ethics committee of our hospital. This study was conducted in accordance with the

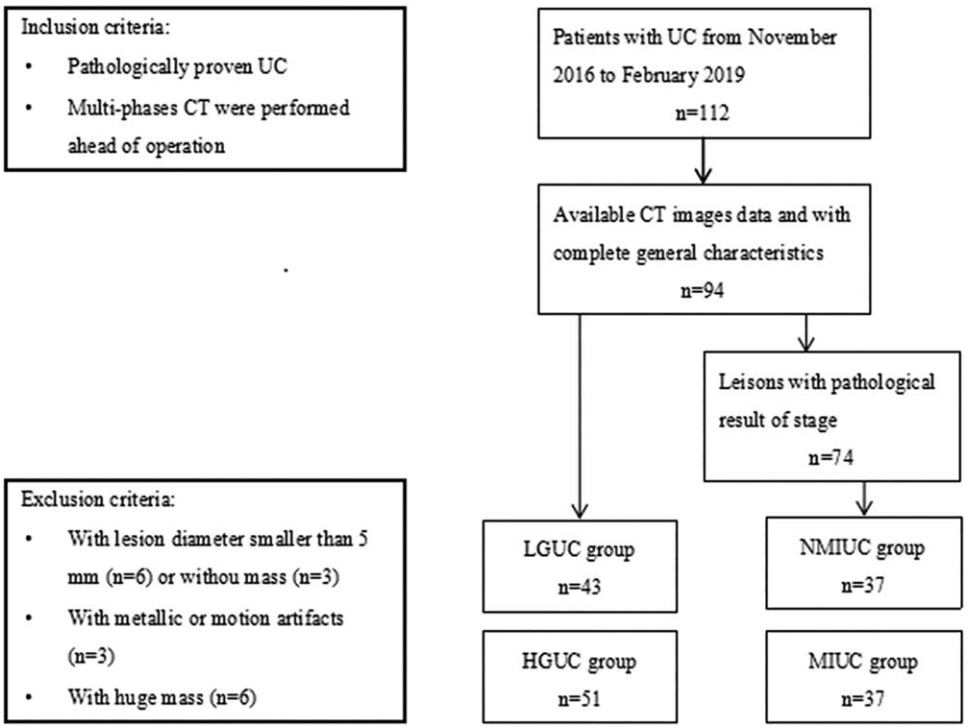


**Figure 1.** Inclusion and exclusion criteria and sample size. CT = computed tomography, HGUC = high-grade urothelial carcinoma, LGUC = low-grade urothelial carcinoma, MIUC = muscle-invasive urothelial carcinoma, NMIU = nonmuscle-invasive urothelial carcinoma.

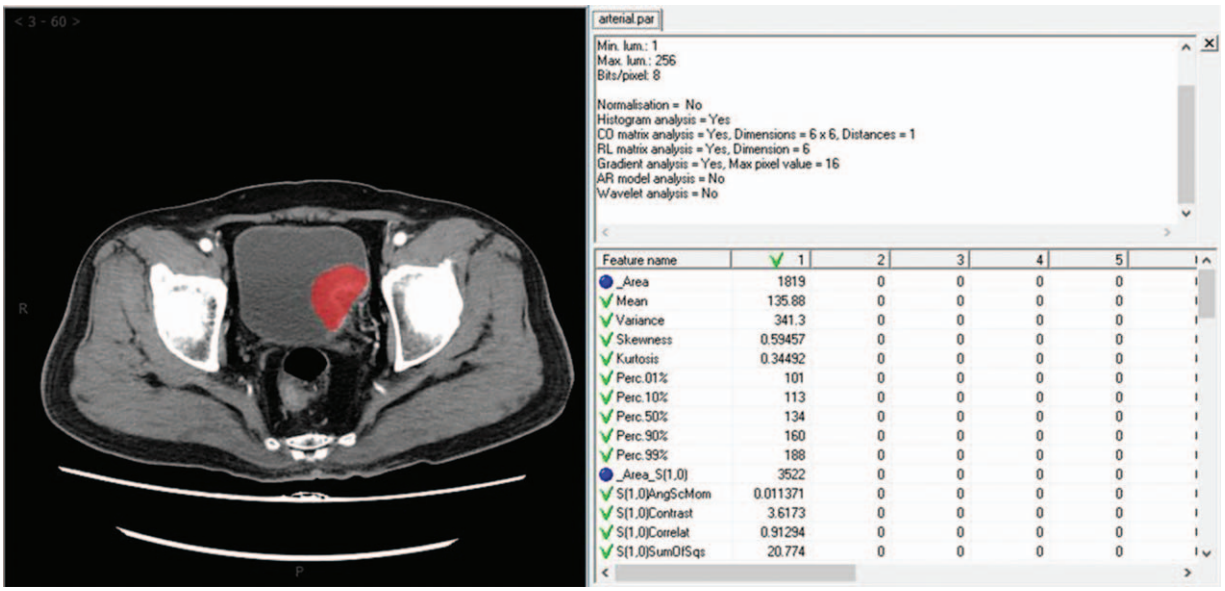


**Figure 2.** Arterial-phase computed tomography images in 52-year-old man with 13-cm high-grade noninvasive urothelial carcinoma in left bladder wall. Region of interest (in red) was segmented within the border of lesion and 78 texture parameters were achieved.

Declaration of Helsinki. Informed consent was not necessary, because the data are anonymized.

### 2.2. CT protocols

All patients in this study underwent contrast-enhanced abdominal and pelvic CT with a 320-slice spiral CT scanner (Aquilion ONE; Canon Medical Systems, Otawara, Japan). Scanning parameters were: tube voltage 120 kVp, 157 mAs, beam collimation $64 \times 0.6$ mm; pitch 0.9; rotation time 0.5 seconds; and reconstruction slice thickness 1 and 7 mm. After unenhanced images (plain CT scan without intravenous contrast) were acquired, a nonionic iodinated contrast agent (Iopamiro, 370 mg/mL; Shanghai Bracco Sine Pharmaceutical Corp Ltd, Shanghai, China) was injected through a dual-head injector at a rate of 3.5 mL/s, followed by a 20 mL normal saline flush with a dose of 2.0 mL/kg bodyweight. Arterial phase, venous phase (VP), and delayed phase (DP) indicate different scanning interval after administration of intravenous contrast. Arterial phase (20–25 seconds), VP (50–60 seconds), and DP (5–8 minutes) images were obtained after injection of contrast in this protocol.

### 2.3. Image selection and export

The CT images for all patients were exported from the picture archiving and communications system workstation in the same format (.bmp) and adjusted to a window width of 360 HU and window level of 60 HU to ensure consistency. DP images were not included because contrast-agent retention in the bladder could cover up lesions, especially small ones, and cause tumor artifacts that would yield false texture parameters.

### 2.4. CT segmentation procedure and texture analysis

The ROI delineation and analysis of texture parameters were performed using MaZda software (version 4.6; Lodz University of Technical, Lodz, Poland). The lesions were objectively measured by tumor ROIs by 2 abdominal radiologists with 10 or 20 years' experience. Two readers were blinded to histopathologic reports about the tumors. ROIs were segmented to give the largest cross-sectional area in all phase images (Fig. 2).

Texture parameters for each image were calculated using MaZda software. These parameters in our study comprised the following features: histogram and gray-level co-occurrence matrix (GLCM). Histogram features were computed from pixel intensity, without considering any spatial relationship between pixels in the original images. This revealed the statistical parameters of histogram distribution, including mean, variance, skewness, kurtosis, and percentiles (1%, 10%, 50%, 90%, and 99%). The use of GLCM with the intensity of pixel pairs described the spatial relationship of 2 pixels in a pair. GLCM features in the MaZda software were angular second moment (AngScMom), contrast, correlation (Correlat), inverse difference moment (InvDfMom), sum of squares (SumOfAqs), sum average (SumAverg), sum variance (SumVarnc), sum entropy (SumEntrp), entropy, difference variance (DifVarnc), and difference entropy (DifEntrp).[19–21] The distances (n = 1) of COM features was used in this study. S(1,0), S(0,1), S(1,1) and S(1,−1) indicated the number of pixel (or pixel neighborhoods) used for parameters computation.

### 2.5. Statistical analysis

IBM SPSS software (version 24.0; IBM Corp, Armonk, NY) was used for statistical analysis. Data normality and homogeneity of variance were examined by Kolmogorov–Smirnov test and Levene test, respectively. If data showed a normal distribution, differences were evaluated using 2-tailed, independent-sample *t* tests. If results were not normally distributed, the Mann–Whitney *U* test was used. Receiver-operating characteristic (ROC) curves were calculated and used to screen CT texture parameters to achieve the optimal cutoff value (threshold). Confidence intervals were kept at 95%, and $P < .05$ was considered statistically significant.

**Table 1**

**The characteristics of patients.**

| | Group 1 | | | Group 2 | | |
|---|---|---|---|---|---|---|
| | **LGUC** | **HGUC** | ***P* value** | **NMIUC** | **MIUC** | ***P* value** |
| Number of patients | 43 | 51 | | 37 | 37 | |
| Gender | | | .802 | | | .693 |
| Male | 39 | 47 | | 33 | 34 | |
| Female | 4 | 4 | | 4 | 3 | |
| Age, years* | 67 ± 12 | 67 ± 10 | .793 | 68 ± 12 | 67 ± 10 | .688 |
| Tumor diameter, mm* | 27.9 ± 15.1 | 33.5 ± 17.1 | .111 | 25.3 ± 14.2 | 35.8 ± 18.1 | **.007** |

HGUC = high-grade urothelial carcinoma, LGUC = low-grade urothelial carcinoma, NMIU = nonmuscle-invasive urothelial carcinoma, MIUC = muscle-invasive urothelial carcinoma.

* Data are mean ± standard deviation.

Statistically significant value shows in bold.

## 3. Results

### 3.1. Patient characteristics

According to the methodologic criteria and pathologic results, 43 LGUC and 51 HGUC were included in group 1, and then subdivided into 37 NMIUC and 37 MIUC (group 2). Statistical results for general patient characteristics in the 2 groups are listed in Table 1. Tumor diameter for NMIUC was significantly smaller than that for MIUC ($P < .05$).

### 3.2. Texture analysis

A total of 78 features were extracted from each phase CT scan, and 26 (33%), 20 (26%), and 22 (28%) texture parameters were significant for differentiating LGUC from HGUC on unenhanced, arterial-phase, and venous-phase CT, respectively. Correspondingly, with 3-phase CT, 19 (24%), 16 (21%), and 30 (38%) texture parameters were statistically significant for differentiating NMIUC from MIUC on unenhanced, arterial-phase, and venous-phase CT. Detailed parameters above were reported in Supplementary Tables S1 and S2, http://links.lww.com/MD/E149.

Based on all the significant features extracted from multiphase CT images, we selected the top 3 radiomic features in unenhanced, arterial, and venous images using ROC curves, as shown in Figure 3 and Tables 2 and 3. The highest area under the curve (AUC) of 0.761 (95% confidence interval [CI] 0.662–0.860) was achieved by S(0,1)SumVarnc at VP for identifying grading, the corresponding diagnostic performance were as follows: sensitivity (Se) = 76.47%, specificity (Sp) = 72.09%, positive predictive value (PPV) = 73.26%, negative predictive value (NPV) = 75.39%. In addition, the highest AUC of 0.798 was obtained by S(0,1)Correlat (95% CI 0.697–0.900) and S(1,1)Correlat (95% CI 0.694–0.902) at VP for determining invasive properties in UC. The corresponding diagnostic performance of S(0,1)Correlat was as follows: Se = 72.97%, Sp = 75.68%, PPV = 75.00%, NPV = 73.68%. The corresponding diagnostic performance of S(1,1)Correlat was as follows: Se = 86.49%, Sp = 67.59%, PPV = 72.73%, NPV = 83.34%.

## 4. Discussion

Several studies reported some biomarkers such as inflammatory markers, circulating tumor cells, and certain RNA have the potential role in predicting prognosis of UC.[22–26] However, using texture analysis to quantitatively analyze multiphase CT images in our study provided us with an alternative way to assess UC grading and invasive properties before pathologic examination. Such objective evaluation, without considering the visual characterization of images, could give physicians some significant information to facilitate clinical management. Our study showed that texture parameters could reflect image heterogeneity,[27] and could be used to improve diagnosis, predict clinical prognosis, and even predict toxicity from relevant treatment.[28–30] Thus, CT texture analysis is a viable method for describing the heterogeneity of UC.

A recent study[17] indicated that UC differentiation could be improved with multiple magnetic resonance sequences. Based on this approach, and opinion, our study tried to enhance

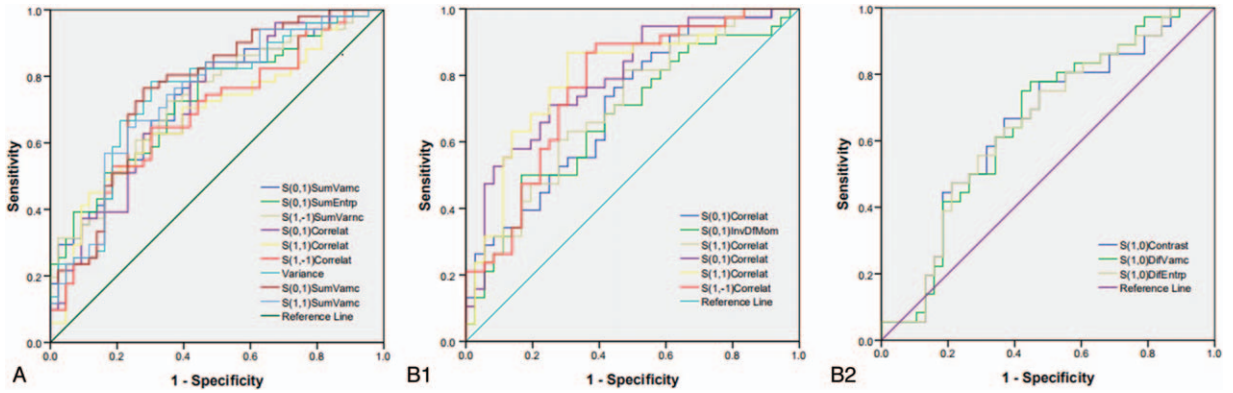


**Figure 3.** Receiver-operating characteristic curves of the top three radiomic features: (A) for low-grade urothelial carcinoma and high-grade urothelial carcinoma; and (B, C) for nonmuscle-invasive urothelial carcinoma and muscle-invasive urothelial carcinoma.

**Table 2**

**Receiver-operating characteristic curves of top 3 texture parameters for differentiating low-grade urothelial carcinoma from high-grade urothelial carcinoma on 3-phase computed tomography images.**

| Phase | Parameters | AUC | 95% CI | *P* value |
|---|---|---|---|---|
| Unenhanced phase | S(0,1)SumVarnc | 0.734 | 0.634–0.834 | <.001 |
| | S(0,1)SumEntrp | 0.727 | 0.626–0.828 | <.001 |
| | S(1,−1)SumVarnc | 0.729 | 0.628–0.830 | <.001 |
| Arterial phase | S(0,1)Correlat | 0.715 | 0.611–0.820 | <.001 |
| | S(1,1)Correlat | 0.686 | 0.579–0.794 | <.01 |
| | S(1,−1)Correlat | 0.680 | 0.572–0.789 | <.01 |
| Venous phase | Variance | 0.745 | 0.643–0.846 | <.001 |
| | S(0,1)SumVarnc | 0.761 | 0.662–0.860 | <.001 |
| | S(1,1)SumVarnc | 0.741 | 0.640–0.843 | <.001 |

AUC = area under curve, CI = confidence interval, Correlat = correlation, SumVarnc = sum variance, SumEntrp = sum entropy.

differentiation by using multiphase CT images to find more significant parameters when diagnosing UC.

In group 1, the top 3 texture parameters, with AUC values of 0.745, 0.761, and 0.741, were all obtained by venous-phase CT. This result demonstrated that variance in venous-phase CT seemed to be the most valuable measure for distinguishing LGUC from HGUC; however, this was a different opinion from a previous study,[18] which did not discuss the impact of multiphase CT images. Nonetheless, other studies[7,31,32] reported the application of contrast-enhanced CT texture analysis in other pathologies. So, whether these differences are due to scan protocol or workflow should be verified in further research. The best diagnostic parameter, S(0,1)SumVarnc, was quantified on venous-phase image. As for diagnostics performance, the parameters of S(0,1)SumVarnc, Se (76.47%), Sp(72.09%), PPV(73.26%), and NPV (75.39%) were not high enough and posted a moderate performance. However, our results demonstrate that texture analysis is feasible solution for differentiating UC.

In group 2, tumor diameter indicating that larger lesions were associated more with MIUC, which is consistent with previous research.[17] Additionally, the optimal parameters, S(0,1)Correlat and S(1,1)Correlat, were acquired in venous-phase CT. However, the unenhanced and arterial-phase CT images were relatively poor predictors of tumor invasiveness. As for diagnostics performance, the parameters of S(1,1)Correlat, Se (86.49%), and NPV (83.34%) showed a relatively good performance, whereas other parameters, Sp (67.59%), PPV (72.73%) and the parameters of S(0,1)Correlat, were not quite satisfactory. The high sensitivity could be explained that if a lesion was predicted with MIUC by texture analysis, the possibility of the lesion with a true MIUC was high.

Variance is a measure of heterogeneity and places high importance on matrix elements that differ from the mean, and on the gray-level variability of pixel pairs, which rises when gray-scale values vary from their means.[33] Correlation, which measures the gray-level linear dependency of adjacent pixels or specified points, could reflect local gray-level dependency of texture images.[33] Our results, which endorse the diagnostic efficiency of variance and correlation, can be explained by the different tumor classifications and tumor heterogeneity, and indicate that quantitative texture analysis could be a feasible device for differentiating UC.

Our study has some limitations. First, the sample size could have been expanded by searching previous records and cooperating with other medical institutions. High-quality, multicenter studies are now required to confirm our results. Second, most LGUC lesions were associated with NMI, while HGUC lesions were generally associated with MI, which may have reduced or confounded the efficacy of UC differentiation; however, we maintain that this problem can be addressed by enlarging sample size. Third, the incidence rate of UC in men is significantly higher than women in our study. It may be contributed to the small sample size and men are also susceptible population of UC due to cigarette smoking in our country. Fourth, relatively few statistically significant vs nonsignificant parameters were identified, and much redundant data were produced, which created a challenge that may have reduced diagnostic efficiency. Lastly, all radiomic analyses involve a few fixed steps, which introduce the drawback of potentially

**Table 3**

**Receiver-operating characteristic curves of top three texture parameters for differentiating nonmuscle-invasive urothelial carcinoma from muscle-invasive urothelial carcinoma on 3-phase computed tomography images.**

| Phase | Parameters | AUC | 95% CI | *P* value |
|---|---|---|---|---|
| Unenhanced phase | S(0,1)Correlat | 0.679 | 0.557–0.801 | <.01 |
| | S(0,1)InvDfMom | 0.652 | 0.527–0.777 | <.05 |
| | S(1,1)Correlat | 0.679 | 0.557–0.801 | <.01 |
| Arterial phase | S(1,0)Contrast | 0.636 | 0.507–0.764 | <.05 |
| | S(1,0)DifVarnc | 0.642 | 0.514–0.770 | <.05 |
| | S(1,0)DifEntrp | 0.638 | 0.511–0.766 | <.05 |
| Venous phase | S(0,1)Correlat | 0.798 | 0.697–0.900 | <.001 |
| | S(1,1)Correlat | 0.798 | 0.694–0.902 | <.001 |
| | S(1,−1)Correlat | 0.781 | 0.674–0.888 | <.001 |

AUC = area under curve, CI = confidence interval, DifEntrp = difference entropy, DifVarnc = difference variance, InvDfMom = inverse difference moment.

dissimilar outcomes due to redundant and nonreproducible parameters.[34,35] Even in multicenter studies, tight scan protocols may be required to minimize this problem.[36]

In conclusion, CT texture analysis in UC is a promising tool for identifying differences in tumor grading and invasiveness. Such analysis has the advantage of being a nontraumatic examination method, independent of the opinion or experience of radiologists, that still permits the accurate diagnosis of patients with cancer.

## Acknowledgment

The authors express their gratitude to Cuihua Zhang for general support in this research.

## Author contributions

**Conceptualization:** Zihua Wang.
**Data curation:** Zihua Wang, Yufang He, Nianhua Wang, Ting Zhang.
**Formal analysis:** Hongzhen Wu.
**Investigation:** Zihua Wang, Yufang He, Nianhua Wang, Ting Zhang.
**Methodology:** Hongzhen Wu, Lei Mo, Xinqing Jiang.
**Project administration:** Zihua Wang, Hongzhen Wu, Lei Mo.
**Resources:** Zihua Wang.
**Software:** Zihua Wang, Yufang He, Nianhua Wang, Ting Zhang.
**Supervision:** Lei Mo, Xinqing Jiang.
**Writing – original draft:** Zihua Wang.
**Writing – review & editing:** Hongzhen Wu, Lei Mo, Xinqing Jiang.

## References

[1] Bray F, Ferlay J, Soerjomataram I, et al. Global cancer statistics 2018: GLOBOCAN estimates of incidence and mortality worldwide for 36 cancers in 185 countries. CA Cancer J Clin 2018;68:394–424.
[2] Sanli O, Dobruch J, Knowles MA, et al. Bladder cancer. Nat Rev Dis Primers 2017;3:17022.
[3] Sylvester RJ, van der Meijden A, Witjes JA, et al. High-grade Ta urothelial carcinoma and carcinoma in situ of the bladder. Urology 2005;66(Suppl 1):90–107.
[4] Humphrey PA, Moch H, Cubilla AL, et al. The 2016 WHO classification of tumours of the urinary system and male genital organs-part B: prostate and bladder tumours. Eur Urol 2016;70:106–19.
[5] Babjuk M, Bohle A, Burger M, et al. EAU guidelines on non-muscle-invasive urothelial carcinoma of the bladder: update 2016. Eur Urol 2017;71:447–61.
[6] Smith AK, Stephenson AJ, Lane BR, et al. Inadequacy of biopsy for diagnosis of upper tract urothelial carcinoma: implications for conservative management. Urology 2011;78:82–6.
[7] Mule S, Thiefin G, Costentin C, et al. Advanced hepatocellular carcinoma: pretreatment contrast-enhanced CT texture parameters as predictive biomarkers of survival in patients treated with sorafenib. Radiology 2018;288:445–55.
[8] Schieda N, Lim RS, Krishna S, et al. Diagnostic accuracy of unenhanced CT analysis to differentiate low-grade from high-grade chromophobe renal cell carcinoma. Am J Roentgenol 2018;210:1079–87.
[9] Varghese BA, Chen F, Hwang DH, et al. Differentiation of predominantly solid enhancing lipid-poor renal cell masses by use of contrast-enhanced CT: evaluating the role of texture in tumor subtyping. AJR Am J Roentgenol 2018;211:W288–96.
[10] Canellas R, Burk KS, Parakh A, et al. Prediction of pancreatic neuroendocrine tumor grade based on CT features and texture analysis. AJR Am J Roentgenol 2018;210:341–6.
[11] Ganeshan B, Panayiotou E, Burnand K, et al. Tumour heterogeneity in non-small cell lung carcinoma assessed by CT texture analysis: a potential marker of survival. Eur Radiol 2012;22:796–802.
[12] Gopalakrishnan V, Yao J, Steagall WK, et al. Use of CT imaging to quantify progression and response to treatment in lymphangioleiomyomatosis. Chest 2019;155:962–71.
[13] Nakajo M, Kajiya Y, Tani A, et al. A pilot study for texture analysis of (18)F-FDG and (18)F-FLT-PET/CT to predict tumor recurrence of patients with colorectal cancer who received surgery. Eur J Nucl Med Mol Imaging 2017;44:2158–68.
[14] Coroller TP, Grossmann P, Hou Y, et al. CT-based radiomic signature predicts distant metastasis in lung adenocarcinoma. Radiother Oncol 2015;114:345–50.
[15] Cha KH, Hadjiiski L, Chan HP, et al. Bladder cancer treatment response assessment in CT using radiomics with deep-learning. Sci Rep 2017;7:8738.
[16] Garapati SS, Hadjiiski L, Cha KH, et al. Urinary bladder cancer staging in CT urography using machine learning. Med Phys 2017;44:5814–23.
[17] Xu X, Zhang X, Tian Q, et al. Quantitative identification of nonmuscle-invasive and muscle-invasive bladder carcinomas: a multiparametric MRI radiomics analysis. J Magn Reson Imaging 2019;49:1489–98.
[18] Zhang GMY, Sun H, Shi B, et al. Quantitative CT texture analysis for evaluating histologic grade of urothelial carcinoma. Abdom Radiol 2016;42:561–8.
[19] Szczypinski PM, Strzelecki M, Materka A, et al. MaZda–a software package for image texture analysis. Comput Methods Programs Biomed 2009;94:66–76.
[20] Yan L, Liu Z, Wang G, et al. Angiomyolipoma with minimal fat: differentiation from clear cell renal cell carcinoma and papillary renal cell carcinoma by texture analysis on CT images. Acad Radiol 2015; 22:1115–21.
[21] Huang Z, Li M, He D, et al. Two-dimensional texture analysis based on CT images to differentiate pancreatic lymphoma and pancreatic adenocarcinoma: a preliminary study. Acad Radiol 2019;26:e189–95.
[22] Cantiello F, Russo GI, Vartolomei MD, et al. Systemic inflammatory markers and oncologic outcomes in patients with high-risk non-muscle-invasive urothelial bladder cancer. Eur Urol Oncol 2018;1:403–10.
[23] Vartolomei MD, Ferro M, Cantiello F, et al. Validation of neutrophil-to-lymphocyte ratio in a multi-institutional cohort of patients with T1G3 non-muscle-invasive bladder cancer. Clin Genitourin Cancer 2018;16: 445–52.
[24] Busetto GM, Ferro M, Del Giudice F, et al. The prognostic role of circulating tumor cells (CTC) in high-risk non-muscle-invasive bladder cancer. Clin Genitourin Cancer 2017;15:e661–6.
[25] Terracciano D, Ferro M, Terreri S, et al. Urinary long noncoding RNAs in nonmuscle-invasive bladder cancer: new architects in cancer prognostic biomarkers. Transl Res 2017;184:108–17.
[26] Ferro M, De Cobelli O, Buonerba C, et al. Modified Glasgow prognostic score is associated with risk of recurrence in bladder cancer patients after radical cystectomy: a multicenter experience. Medicine (Baltimore) 2015; 94:e1861.
[27] Miles KA, Ganeshan B, Hayball MP. CT texture analysis using the filtration-histogram method: what do the measurements mean? Cancer Imaging 2013;13:400–6.
[28] Skogen K, Schulz A, Dormagen JB, et al. Diagnostic performance of texture analysis on MRI in grading cerebral gliomas. Eur J Radiol 2016;85:824–9.
[29] Hunter LA, Chen YP, Zhang L, et al. NSCLC tumor shrinkage prediction using quantitative image features. Comput Med Imaging Graph 2016; 49:29–36.
[30] Mattonen SA, Palma DA, Haasbeek CJ, et al. Distinguishing radiation fibrosis from tumour recurrence after stereotactic ablative radiotherapy (SABR) for lung cancer: a quantitative analysis of CT density changes. Acta Oncol 2013;52:910–8.
[31] D'Onofrio M, Ciaravino V, Cardobi N, et al. CT enhancement and 3D texture analysis of pancreatic neuroendocrine neoplasms. Sci Rep 2019; 9:2176.
[32] Deng Y, Soule E, Samuel A, et al. CT texture analysis in the differentiation of major renal cell carcinoma subtypes and correlation with Fuhrman grade. Eur Radiol 2019;29:6922–9.
[33] Yang X, Tridandapani S, Beitler JJ, et al. Ultrasound GLCM texture analysis of radiation-induced parotid-gland injury in head-and-neck cancer radiotherapy: an in vivo study of late toxicity. Med Phys 2012;39:5732–9.
[34] Hatt M, Tixier F, Pierce L, et al. Characterization of PET/CT images using texture analysis: the past, the present... any future? Eur J Nucl Med Mol Imaging 2017;44:151–65.
[35] Yip SS, Aerts HJ. Applications and limitations of radiomics. Phys Med Biol 2016;61:R150–66.
[36] Berenguer R, Pastor-Juan MDR, Canales-Vazquez J, et al. Radiomics of CT features may be nonreproducible and redundant: influence of CT acquisition parameters. Radiology 2018;288:407–15.